Journal of Solid State Chemistry 182 (2009) 3387–3392

Contents lists available at ScienceDirect

Journal of Solid State Chemistry

journal homepage: www.elsevier.com/locate/jssc

Efficient preparation of nanocrystalline anatase TiO_2 and V/TiO_2 thin layers using microwave drying and/or microwave calcination technique

H. Žabová [a,*], J. Sobek [a], V. Církva [a], O. Šolcová [a], Š. Kment [b], M. Hájek [a]

[a] Institute of Chemical Process Fundamentals, Academy of Sciences of the Czech Republic, v.v.i., Rozvojová 135, 165 02 Prague 6, Czech Republic
[b] Institute of Physics, Academy of Sciences of the Czech Republic, Na Slovance 2, 182 21 Prague 8, Czech Republic

ARTICLE INFO

Article history:
Received 11 August 2009
Received in revised form
16 September 2009
Accepted 20 September 2009
Available online 12 October 2009

Keywords:
Thin layers
V-doped titanium dioxide
Microwaves
Photocatalysis

ABSTRACT

This study has demonstrated that the synthesis of TiO_2 and V/TiO_2 thin layers may be significantly improved and extended if microwave energy is employed during the drying and/or calcination step. Thin nanoparticulate titania layers were prepared via the sol–gel method using titanium *n*-butoxide as a precursor. As prepared films were then analyzed by means of various characterization techniques (Raman spectroscopy, UV/Vis, AFM, XPS) in order to determine their functional properties. The photocatalytic activities of prepared layers were quantified by the decoloring rate of Rhodamine B. All thermal treatments in microwave field were done in the same manner, by using an IR pyrometer in the microwave oven and monitoring the temperature of the heating. Nevertheless the microwave and thermally prepared materials were different. This in turn may lead to differences in their functional and also photocatalytic properties.

1. Introduction

There has been a great deal of interest of nanoparticulate titanium dioxide thin films synthesized by means of the sol–gel method. Nanostructured TiO_2 thin films have many important applications, including, among others, dye-sensitized solar cells [1] or photocatalytic decomposition of various organic molecules [2–5]. Sol–gel processing of titanium dioxide has been investigated since the 19th century and nowadays modern techniques have been developed to control the precursor stability and phase formation. Also, the sol–gel method within templates of surfactants assemblies organized as reverse micelles was studied in order to obtain numerous new materials with regular and controlled morphology. Compared to other methods the surfactant mediated sol–gel provides a good control of the hydrolysis rate [6]. Sol–gel method has several advantages such as low processing temperature, homogeneity, possibility of coating on larger area substrates and cost effective. Since the sol–gel method is a solution process, it has all the advantages of wet chemical process that are important in preparation of doped TiO_2 layers, such as control of stoichiometry, doping of desired amount of transition metal ions and fine dispersion of the dopant and titanium source [7]. Doping with transition metal ions prolongs the light absorption of TiO_2 to the visible region and it is also able to enhance interfacial charge-transfer reactions, thus increasing the photocatalytic properties of TiO_2 [8]. For example, vanadium has been found as an effective dopant by many research groups [9,10]. Wu et al. [11] found that a visible-light response TiO_2 catalyst via vanadium doping promoted the particle growth and enhanced "red-shift" in the UV/Vis absorption spectra. They concluded vanadium to be highly dispersed inside the titania structure by XAS analysis and also evaluated the higher photocatalytic activity of V/TiO_2. The sol–gel derived precipitates requiring further heat treatment at a high temperature to induce crystallization. The calcination process may gives rise to particle agglomeration and grain growth and hence induce undesirable phase transformation [12].

Microwave energy has been employed in many recent chemical reaction studies and has been found to change the kinetics and selectivity, often in favorable ways [13–15]. Microwave energy is found to be more efficient in the selective heating in many processes. These processes are understood to be more environmentally friendly, requiring less energy than conventional processes [16]. One of the most exciting areas where microwave energy has been demonstrated to influence reaction is rightly the synthesis of nanoporous materials (powders or layers). Despite the fact that microwave technique offers a clean, cost effective, energy effective and convenient method of heating, the main advantages of this process are reduced time required for synthesis, dimension uniformity of product and variability of product composition [17]. Conventional heating may cause sintering of material as a conduction process. That is, heat is deposited on the outside of the object and diffuses inward by conduction [18]. On the other hand, microwave heating is generated uniformly throughout the material, resulting in uniform sintering of the material, the required temperature and time

* Corresponding author. Fax: +420 220920661.
E-mail address: zabova@icpf.cas.cz (H. Žabová).

0022-4596/$ - see front matter © 2009 Elsevier Inc. All rights reserved.
doi:10.1016/j.jssc.2009.09.033

is often reduced, grain growth is suppressed [19]. Microwave heating may also reduce the extent of nanoparticles growing, leading to a TiO_2 thin film with higher surface area and, consequently, higher photocatalytic efficiency [20].

In this work, different types of TiO_2 and V/TiO_2 colloids (conventional heat treatment, microwave heat treatment and microwave drying) were immobilized on microscopic slides, resulting in TiO_2 thin layers. The functional and photocatalytic behavior of the corresponding TiO_2 layers is presented. The aim was to establish whether differences between the two heating and drying techniques may be useful in the production of nanoparticulate TiO_2 thin layers with other structural, morphological and optical properties.

2. Experimental

2.1. Materials

Titanium *n*-butoxide (97%), acetylacetone (99.5%), ethyl alcohol (99%) and hydrochloric acid were used as obtained (all from Sigma Aldrich, Prague, CR) for the titanium dioxide preparation. Vanadyl acetylacetonate (Sigma Aldrich, 98%) was used for preparation of vanadium doped titanium dioxide. Rhodamine B (Lachema, Brno, CR) was used as received for photocatalytic experiments. All solutions were prepared using distilled water ($1\,\mu S\,cm^{-1}$).

2.2. Preparation of TiO_2 and V/TiO_2 thin layers

The TiO_2 photocatalyst was prepared via sol–gel method using titanium *n*-butoxide (10 mL) as a molecular precursor of TiO_2 as we described in our previous work [21]. The hydrolysis of alkoxide was carried out in the environment of acetylacetone (10 mL) and ethyl alcohol (10 mL) as solvents. The resulting reaction originated a solution, into which the water (4 mL) and hydrochloric acid (0.5 mL) were added dropwise under mechanical stirring. For vanadium doped TiO_2 photocatalyst, the procedure was the same, only appropriate amount of vanadyl acetylacetonate (0.3 g) was initially dissolved in acetylacetone.

Prior to the layer deposition, the supports (microscopic slides, $75 \times 25 \times 1$ mm, Superior Marienfeld) were thoroughly cleaned (water–soap mixture, solution of hydrochloric acid, distilled water and ethanol). The TiO_2 layer was prepared by dip-coating of the supports into the gel with withdrawal rate of $6\,cm\,min^{-1}$. The layers were then dried in air at ambient temperature for one hour or dried in a laboratory microwave oven (MicroSYNTH Labstation, Milestone, Italy, 2450 MHz) for 6 min. Finally, the dried layers were thermally treated by conventional heating in electrical furnace at 500 °C for 2 h ($2\,^{\circ}C\,min^{-1}$) or treated by microwave heating in laboratory microwave oven for 10 min. Microwave treatments were performed using silicon carbide as a susceptor to provide indirect heating of layers. Carbide wafers were used because of its high efficiency in microwave absorption (ε_r=6.52). The as deposited thin layers were placed into an alumina crucible (length of 8 and 5 cm in diameter) in which carbide wafers and insulation material were located. The temperature of heating inside the crucible was measured using an IR pyrometer (Raytek, USA).

2.3. Characterization of TiO_2 and V/TiO_2 thin layers

Raman spectra were recorded in order to examine the crystallographic phase of titanium dioxide. Analyses were carried out on dispersive Raman spectrograph (Nicolet Almega XR, Thermo Scientific, USA) with laser wavelength of 473 nm, laser power 100%, objective 50 × and pinhole 100 μm.

Relative surface roughness and topographical features of the TiO_2 and V/TiO_2 layers were measured by atomic force microscopy using an AFM Explorer (ThermoMicroscopes, Sunnyvale, USA).

The UV/Vis spectrophotometer (Shimadzu, UV-2450, Japan) was employed for detecting absorption edges of the prepared layers in the spectral range from 200 to 800 nm.

X-ray photoelectron spectroscopy measurements were performed by an ESCA Probe P photoelectron spectrometer (Omicron Nanotechnology Ltd., Taunusstein, Germany) using monochromatic Al*K*α X-ray source with energy of 1486.7 eV and pressure 10^{-10} mbar. Contamination species were not observed apart from the adsorbed atmospheric carbon (C 1 s binding energy value of 284.7 eV).

2.4. Photocatalytic experiments

Photocatalytic activity of pristine and doped TiO_2 under UV irradiation was characterized by the test of Rhodamine B (RhB, $C_{28}H_{31}ClN_2O_3$) decolorization rate. The sample of TiO_2 layer was vertically placed in a glass reactor (cuvette, $30 \times 50 \times 10$ mm) containing 10 mL of RhB solution with initial concentration of $10^{-4}\,mol\,L^{-1}$. After 15 min in the dark, the solution was irradiated. The UV light was provided by a 400 W high-pressure mercury lamp (HQL 400 W; Osram, Munich, Germany) for 90 min. The absorbance of RhB at the wavelength of 553 nm was used as an indicator for the photoreactivity tests (Helios γ; Thermo Electron Corporation; software Vision 32). Since the Rhodamine B is present in trace concentration ($K \cdot c \ll 1$) the Langmuir–Hinshelwood model simplifies to a pseudo-first-order kinetic equation [22]:

$$\ln \frac{c_0}{c} = k \cdot K \cdot t = k_{app} \cdot t$$

where c_0 is the initial RhB concentration, c the RhB concentration in time t, t the illumination time, k the reaction rate constant, K the adsorption coefficient of RhB and k_{app} the apparent rate constant.

3. Results and discussion

Raman spectroscopy studies revealed that TiO_2 layers, conventional treated and also microwave treated, have anatase crystallographic structure and show almost all of the expected vibrational modes, correlating with literature on Raman spectrum of anatase TiO_2 (A_{1g}+$2B_{1g}$+$3E_g$) [23]. Raman spectra for undoped titanium dioxide layers, S1 (air dried and conventionally treated), S2 (microwave dried and conventionally treated) and S3 (air dried and microwave treated), are shown in Fig. 1. Well-resolved anatase peaks were observed in the spectra of all samples, indicating that anatase nanoparticles are the predominant species. For example, the Raman peaks assigned to sample S1 were indicated at $141\,cm^{-1}$ (E_g), $197\,cm^{-1}$ (E_g), $398\,cm^{-1}$ (B_{1g}), $515\,cm^{-1}$ (B_{1g}) and $640\,cm^{-1}$ (E_g), except A_{1g} mode, which was suppressed by stronger peak at $515\,cm^{-1}$ (B_{1g}). We can also recognize a very few Raman peaks assigned to brookite phase ($6A_{1g}$+$6B_{1g}$+$4B_{2g}$+B_{3g}) of TiO_2 [24]: $243\,cm^{-1}$ (A_{1g}), $312\,cm^{-1}$ (B_{1g}) for sample S1; $241\,cm^{-1}$ (A_{1g}) for sample S2 and $243\,cm^{-1}$ (A_{1g}) for sample S3. No effects of dopant were observed on the position of Raman peaks in the spectra of vanadium doped titanium dioxide thin layers, S4 (air dried and conventionally treated), S5 (microwave dried and conventionally treated) and S6 (air dried and microwave treated), depicted in Fig. 2. The Raman peaks for sample S4 were observed at $143\,cm^{-1}$ (E_g), $196\,cm^{-1}$ (E_g),

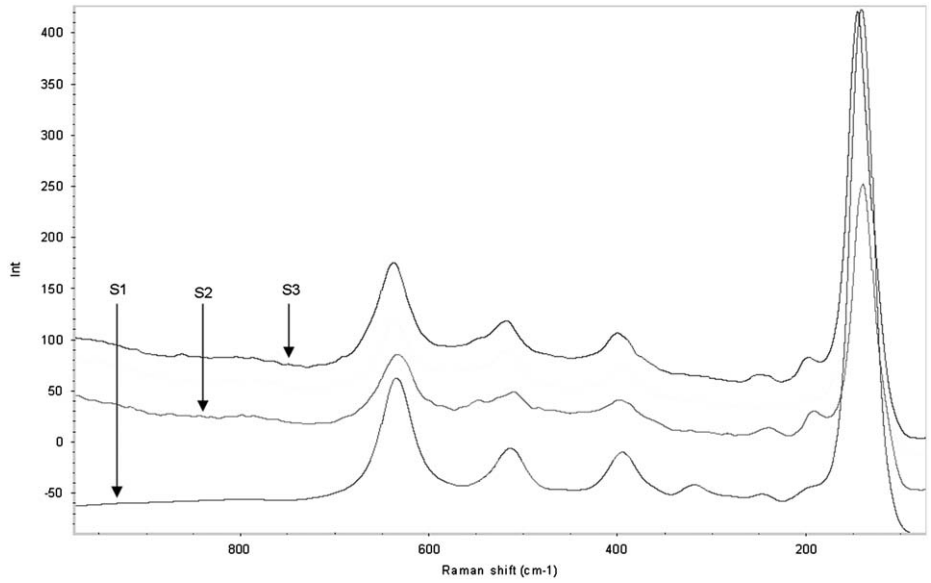

Fig. 1. Raman spectra of TiO_2 thin layers: S1-air dried and conventionally treated layer, S2-microwave dried and conventionally treated layer, and S3-air dried and microwave treated layer.

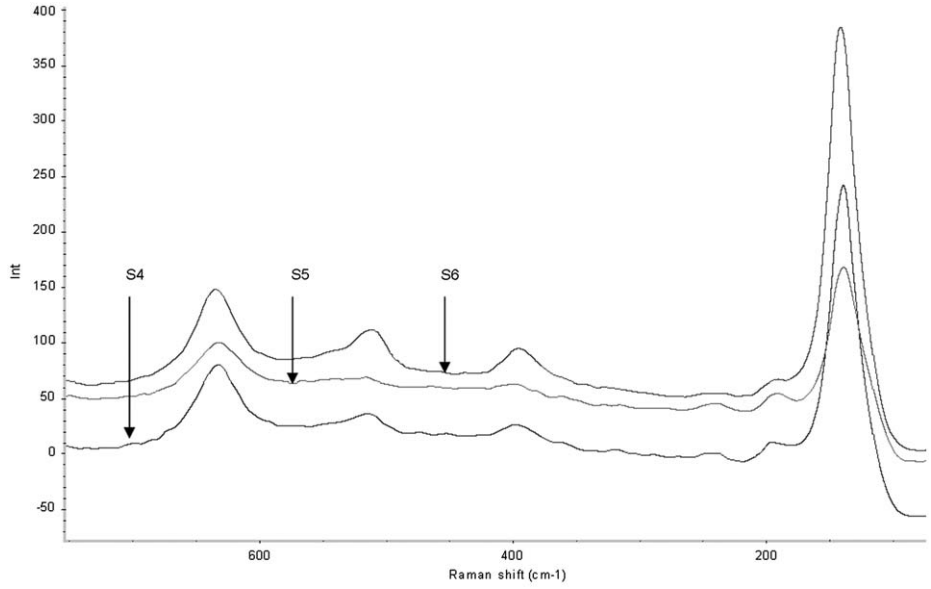

Fig. 2. Raman spectra of V/TiO_2 thin layers: S4-air dried and conventionally treated layer, S5-microwave dried and conventionally treated layer, and S6-air dried and microwave treated layer.

395 cm^{-1} (B_{1g}), 519 cm^{-1} (B_{1g}) and 638 cm^{-1} (E_g). It means that anatase structure is retained after doping and dopant may occupy the substitutional sites in the host lattice [25]. However, we can find more brookite peaks in the Raman spectrum of S4 sample than in S1 sample at A_{1g} (156, 190, 241, 405, 630 cm^{-1}), B_{1g} (314 cm^{-1}), B_{2g} (360, 395, 498, 585 cm^{-1}) and B_{3g} (449 cm^{-1}). This indicates that the presence of vanadium changes a ratio of TiO_2 crystallographic phases. Nevertheless, the presence of brookite phase in the microwave treated sample S6 is suppressed due to the mild microwave treatment technology without deterious effects on the properties of prepared layers.

Relative surface roughness of the TiO_2 and V/TiO_2 thin layers microwave exposed and annealed at 500 °C were measured by atomic force microscopy, which are shown in Fig. 3. Layers exposed to microwaves (S3) and conventionally annealed (S1) showed roughness, calculated from surface area 1×1 μm, 0.56 and 0.48 nm, respectively. These images indicate that there was no significant difference in the structure of TiO_2 layers to which different heat treatments were applied. On the other hand, the difference between air dried (S1) and microwave dried (S2) thin layers was observed. In comparison, an image of the microwave dried layer surface depicts many visible, large and loose aggregates, affording this layer an increased porous structure and also surface roughness (2.51 nm). However, the relative surface roughness and the morphology of the layers produced from the different processes were identified to be different in the case of the preparation of vanadium doped TiO_2 thin layers. This is illustrated in image S5 (2.24 nm), where the surface roughness of the microwave dried layer is comparable to that of the microwave exposed S6 (2.08 nm) and the surfaces

appear smooth and the nanoporous natured. Significant difference between images S4 (4.45 nm) and S6 is the relative packing of nanoparticles. The V/TiO_2 layers produced from microwaves show the nanoparticles as a densely packed structure, while V/TiO_2 aggregates on the conventional treated layers are visible, that is, microwave processed layers are more compact than the conventional treated layers. This structure will result in a large specific surface area. In other words, the more compact structure of microwave treated layers have the largest overall effective surface area for the same geometric film area, or in terms of oxidation capacity, have the largest number of oxidation reaction sites among all the films. So that, using microwaves in preparation of vanadium doped titania thin layers may suppress the grain growth of crystal and improve the distribution of particles and also their organization.

The absorption edges were determined using absorption data of thin layers in the range of 200–800 nm. UV/Vis absorption spectra clearly show (Fig. 4) that the incorporation of vanadium ions into TiO_2 leads to a red shift in the optical response, as well as reduction in the band gap energy. The red shift in absorption spectra is attributed to the transfer of electrons from transition metal ions to the conduction band of TiO_2 [26]. The absorption edges of undoped titanium dioxide thin layers were determined around 365 nm (~3.4 eV). The prepared samples are not ideal materials. There are a lot of defects in crystal structure (mainly O vacancies) that influence absorption edge of the samples of TiO2. A quantum size effect of TiO_2 nanoparticles says that as the particle size decrease the band gap energies increase, i.e. optical absorption threshold for nanocrystallites of this size shifts to higher energies [27]. No significant differences in absorption properties have been observed between layers prepared by various techniques.

To investigate the chemical state of vanadium incorporated into TiO_2, V $2p_{3/2}$ binding energies were studied by measuring the XPS spectra. High resolution XPS spectra of V $2p_{3/2}$ of vanadium doped titanium dioxide layers prepared by different heating technique are shown in Fig. 5a and b. The core level of V $2p_{3/2}$ in microwave treated V/TiO_2 thin layer (S6) show binding energy peak at 516 eV (Fig. 5a) and can be assigned to V^{4+} [28]. Vanadium ions were incorporated into the crystal lattice of TiO_2 and formed Ti–O–V bond but no V–Ti bond was present. The peak of V $2p_{3/2}$ in conventionally treated V/TiO_2 thin layer (S4) appeared as two shoulders (Fig. 5b). The shoulder at a binding energy of 515.6 eV suggests V^{4+} species, whereas the shoulder at 516.7 eV can be assigned to V^{5+}. Since vanadium existed only as V^{4+} in the precursor (as VO^{2+} vanadyl), some V^{4+} ions must be oxidized into V^{5+} during the preparation process, rather during annealing. The V $2p_{3/2}$ small peak obviously interfered with the bigger V $2p_{3/2}$ peak of binding energy 512.6 eV indicated that vanadium is also of

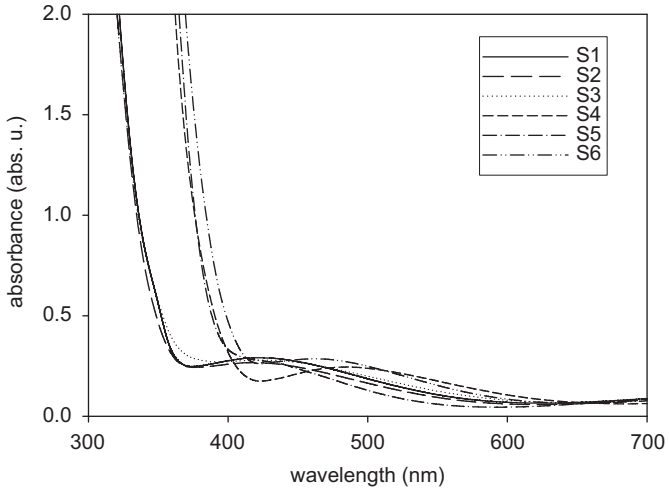

Fig. 4. Absorption properties of TiO_2 and V/TiO_2 thin layers.

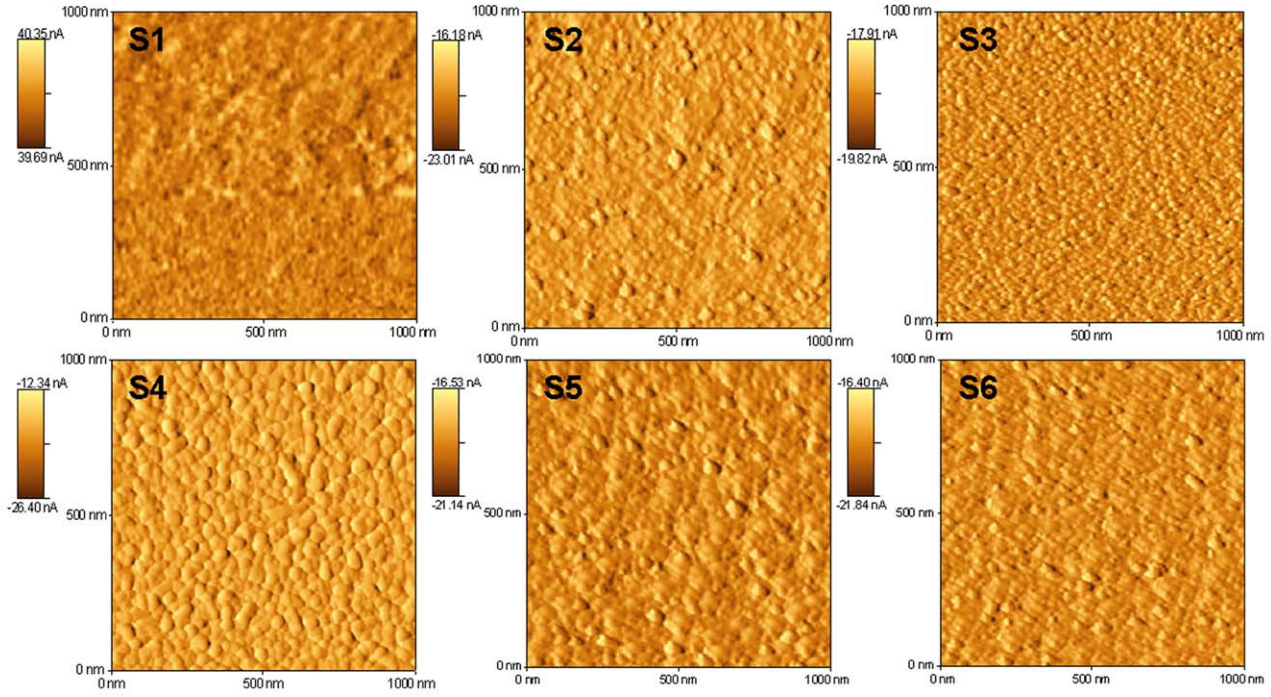

Fig. 3. AFM images.

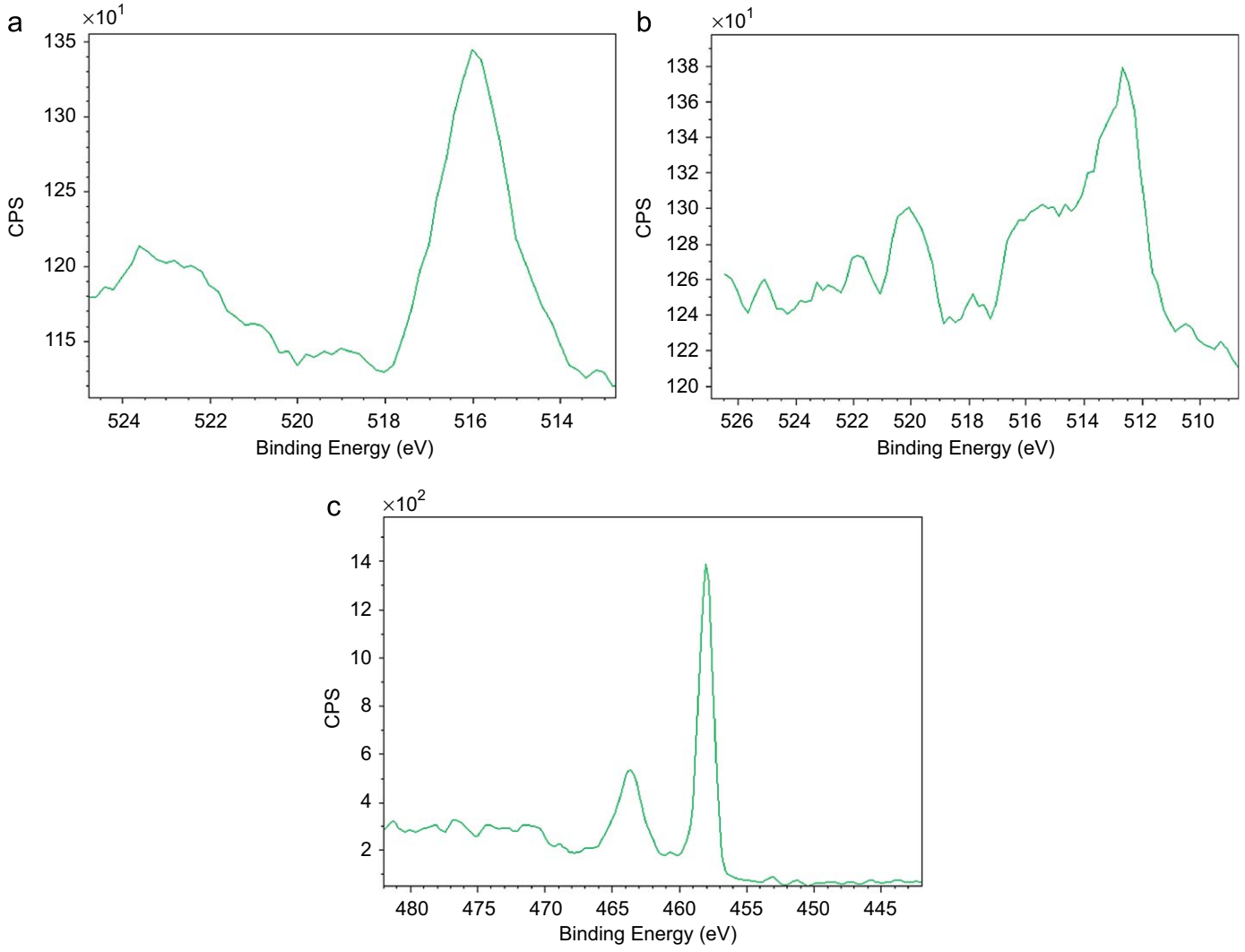

Fig. 5. XPS analysis: (a) V 2*p* spectrum of S6 sample, (b) V 2*p* spectrum of S4 sample, and (c) Ti 2*p* spectrum of S4 sample.

Table 1
The photocatalytic activity of TiO_2 and V/TiO_2 layers prepared by different heating treatment techniques.

Sample	k_{app} (min^{-1})	rms (nm)[a]	Drying time (min)	Annealing time (min)	Annealing temperature (°C)
S1	0.0081	0.48	60[b]	120[d]	500 ± 3[f]
S2	0.0077	2.51	6[c]	120[d]	500 ± 3[f]
S3	0.0088	0.56	60[b]	10[e]	500 ± 3[f]
S4	0.0084	4.45	60[b]	120[d]	500 ± 1[g]
S5	0.0119	2.24	6[c]	120[d]	500 ± 1[g]
S6	0.0136	2.08	60[b]	10[e]	500 ± 1[g]

[a] Relative surface roughness measured by AFM.
[b] Air dried.
[c] Microwave dried.
[d] Conventionally annealed.
[e] Microwave annealed.
[f] Measured by thermocouple in electric furnace.
[g] Measured by IR pyrometer.

metallic nature V^0. The pentavalent state of vanadium was produced by the preparation procedure of the V/TiO_2 layer. The appearance of elementary vanadium may be explained by photon-induced reduction of vanadium ions after exposure to the X-rays during XPS analysis. This phenomenon has been reported in the case of electrochemically prepared Cr/TiO_2 films [29]. Two peaks for the Ti 2*p* in XPS spectrum of pure TiO_2 layer were observed at 464.8 and 459.1 eV and assigned to Ti $2p_{1/2}$ and Ti $2p_{3/2}$, respectively. The peak separation was 5.7 eV indicating the presence of Ti^{4+} (TiO_2) in these layers [30]. The binding energy

peaks of Ti 2p in V/TiO_2 layer were found at 465.1 eV ($2p_{1/2}$) and 459.4 eV ($2p_{3/2}$). The peak separation (5.7 eV) was retained after vanadium doping, but these energy peaks have positive shift of 0.3 eV with comparison to the pure TiO_2. This may indicate positively charged surface of vanadium doped TiO_2 which is due to the presence of metal ions [31].

The photocatalytic activities of pristine and doped TiO_2 obtained from different heating treatment procedures are listed in Table 1. It was founded that the photocatalytic activity of S2 sample was the worst among all pristine samples of TiO_2. It indicates that microwave drying technique is not such suitable for preparation of un-doped titanium dioxide thin layers. On the other hand, microwave treated thin layers of TiO_2 showed a very good photocatalytic activity comparing with conventionally treated layers. These results are in good agreement with relative surface roughness values obtained by atomic force microscopy. In the case of vanadium doped TiO_2 layers, the most active sample was the microwave treated. However, also microwave dried sample showed a high photocatalytic activity. Microwaves may influence the distribution of dopant particles in both cases, during drying and also during final treatment. Better activity of microwave treated V/TiO_2 samples is probably due to their good crystallinity and electron trapping effect of vanadium ions. It may be also caused by the lower absorption threshold.

4. Conclusions

Thin layers of TiO_2 and V/TiO_2 were prepared using microwave drying and microwave calcination technique. Their functional and also photocatalytic properties were compared with conventionally prepared layers. It was dissolved that microwaves may influence the crystallinity of samples, their roughness and also distribution of dopant species. Photocatalytic activity of prepared layers was enhanced in the case of vanadium doped TiO_2 and it was also increased in microwave processed samples. Microwave heating is a complex process and its use introduces challenges to the heat treatment of TiO_2 layers and also other materials. Microwave processing has the potential to reduce the time, cost and required energy input for the production of thin layers. Therefore, this new innovative annealing of thin layers will open a new door for advanced technologies.

Acknowledgements

Authors thank the Grant Agency of the Czech Republic (104/07/1212, 203/08/H032) for funding this research. We are also grateful to Milestone s.r.l. (Italy) for their technical support.

References

[1] B. O'Regan, M. Grätzel, Nature 353 (1991) 737–740.
[2] T.M. Twesme, D.T. Tompkins, M.A. Anderson, T.W. Root, Appl. Catal. B 64 (2006) 153–160.
[3] N. Doucet, O. Zahraa, M. Bouchy, Catal. Today 122 (2007) 168–177.
[4] S. Irmak, E. Kusvuran, O. Erbatur, Appl. Catal. B 54 (2004) 85–91.
[5] I. Dolamic, T. Burgi, J. Phys. Chem. B 110 (2006) 14898–14904.
[6] P. Kluson, H. Luskova, T. Cajthaml, O. Solcova, Thin Solid Films 495 (2006) 18–23.
[7] N. Venkatachalam, M. Palanichamy, B. Arabindoo, V. Murugesan, J. Mol. Catal. A 266 (2007) 158–165.
[8] A. Di Paola, G. Marci, L. Palmisano, M. Schiavello, K. Upsali, S. Ikeda, B. Ohtani, J. Phys. Chem. B 106 (2002) 637–645.
[9] N. Serpone, D. Lawless, Langmuir 10 (1994) 643–652.
[10] J. Chen, M. Yao, X. Wang, J. Nanopart. Res. 10 (2008) 163–171.
[11] J.C.-S. Wu, Ch.-H. Chen, J. Photochem. Photobiol. A 163 (2004) 509–515.
[12] T. Noguchi, A. Fujishima, Environ. Sci. Technol. 32 (1998) 3831–3833.
[13] M. Nüchter, B. Ondruschka, A. Jungnickel, U. Müller, J. Phys. Org. Chem. 13 (2000) 579–586.
[14] P. Lidström, J. Tierney, B. Wathey, J. Westman, Tetrahedron 57 (2001) 9225–9283.
[15] C.O. Kappe, Angew. Chem. Int. Ed. 43 (2004) 6250–6284.
[16] D. Di Claudio, A.R. Phani, S. Santucci, Opt. Mater. 30 (2007) 279–284.
[17] G.A. Tompsett, W.C. Conner, K.S. Yngvesson, Chem. Phys. Chem. 7 (2006) 296–319.
[18] J.H. Booske, J. Mater. Res. 7 (1992) 495–501.
[19] J.N. Hart, D. Menzies, Y.-B. Cheng, G.P. Simon, L. Spiccia, Sol. Energy Mater. Sol. Cells 91 (2007) 6–16.
[20] J.N. Hart, Y.-B. Cheng, G.P. Simon, L. Spiccia, Surf. Coat. Technol. 198 (2005) 20–23.
[21] H. Žabová, V. Církva, J. Chem. Technol. Biotechnol. (2009), doi:10.1002/jctb.2220.
[22] Y. Ao, J. Xu, D. Fu, C. Yuan, Appl. Surf. Sci. 255 (2008) 3137–3140.
[23] T. Ohsaka, F. Izumi, Y. Fujiki, J. Raman Spectrosc. 7 (1978) 321–324.
[24] G.A. Tompsett, G.A. Bowmaker, R.P. Cooney, J.B. Metson, K.A. Rodgers, J.M. Seakins, J. Raman Spectrosc. 26 (1995) 57–62.
[25] A.P. Singh, S. Kumari, R. Shrivastav, S. Dass, V.R. Satsangi, Int. J. Hydrogen Energy 33 (2008) 5363–5368.
[26] Ch.-G. Wu, Ch.-Ch. Chao, F.-T. Kuo, Catal. Today 97 (2004) 103–112.
[27] K.M. Reddy, C.V.G. Reddy, S.V. Manorama, J. Solid State Chem. 158 (2001) 180–186.
[28] X. Yang, Ch. Cao, K. Hohn, L. Erickson, R. Maghirang, D. Hamal, K. Klabunde, J. Catal. 252 (2007) 296–302.
[29] G.P. Halada, C.R. Clayton, J. Electrochem. Soc. 138 (1991) 2921–2927.
[30] S.-K. Joung, T. Amemiya, M. Murabayashi, K. Itoh, Chem. Eur. J. 12 (2006) 5526–5534.
[31] S.D. Sharma, K.K. Saini, Ch. Kant, C.P. Sharma, S.C. Jain, Appl. Catal. B 84 (2008) 233–240.